Deletion of AMPKα1 Attenuates the Anticontractile Effect of Perivascular Adipose Tissue (PVAT) and Reduces Adiponectin Release.

Tarek A.M. Almabrouk[1,2], Azizah B. Ugusman[1], Omar J. Katwan[1,3], Ian P. Salt[1] and Simon Kennedy[1]

1. Institute of Cardiovascular and Medical Sciences, College of Medical, Veterinary & Life Sciences, University of Glasgow, Glasgow, G12 8QQ, U.K.
2. Department of Pharmacology, School of medicine, University of Zawia, Zawia, Libya.
3. Department of Biochemistry, College of medicine, University of Diyala, Iraq.

Corresponding author:

Dr Simon Kennedy, Institute of Cardiovascular and Medical Sciences, College of Medical, Veterinary & Life Sciences, University of Glasgow, Glasgow, G12 8QQ, U.K.

Email: simon.kennedy@glasgow.ac.uk

Tel: +44 (0) 141 330 4763

Keywords: AMPK, perivascular adipose tissue, aorta, adiponectin, anticontractile

Short title: AMPK and PVAT function

Abstract

Background: Perivascular adipose tissue (PVAT) surrounds most blood vessels and secretes numerous active substances, including adiponectin which produce a net anticontractile effect in healthy PVAT. AMP-activated protein kinase (AMPK) is a key mediator of cellular energy balance and may mediate the vascular effects of adiponectin. In this study we investigated the role of AMPK within PVAT in mediating the anticontractile effect of PVAT.

Methods: Endothelium-denuded aortic rings from wild-type (Sv129) and α_1AMPK knockout (KO) mice were mounted on a wire myograph. Dose-response curves to the AMPK-independent vasodilator cromakalim were studied in vessels with and without PVAT and the effect of preincubation with conditioned media (CM) and adiponectin on relaxation also studied. The effect of AMPKα1 KO on the secretory profile of PVAT was assessed by ELISA.

Results: Thoracic aortic PVAT from KO mice was morphologically indistinct from WT and primarily composed of brown adipose tissue. PVAT augmented relaxation to cromakalim in WT but not KO mice. Addition of WT PVAT augmented relaxation in KO aortic rings but KO PVAT had no effect in WT mice. PVAT from KO mice secreted significantly less adiponectin and addition of adiponectin to either KO or WT aortic rings without PVAT augmented relaxation to cromakalim. An adiponectin blocking peptide significantly attenuated relaxation in WT rings with PVAT but not in KO rings.

Conclusion: This study demonstrates that AMPKα1 has a critical role in maintaining the anticontractile actions of PVAT; an effect independent of the endothelium but likely mediated through altered adiponectin secretion or sensitivity.

Abbreviations: PVAT- perivascular adipose tissue; AMPK- AMP-activated protein kinase; WT- wild type; KO- knock-out; WAT- white adipose tissue; BAT- brown adipose tissue; CM- conditioned media; VSMCs- vascular smooth muscle cells; UCP-1- uncoupling protein-1; ACC- Acetyl CoA carboxylase; ADRF- adventitia-derived relaxing factor; sGC- Soluble guanylyl cyclase.

Table of links

TARGETS	
Other protein targets	**Enzymes**
Uncoupling Protein-1 (UCP-1)	**AMPK**
	ACC
Receptor	
Adipo1 receptor (AdipoR1)	

LIGANDS
Adiponectin
A769662
U46619
Cromakalim
AICAR

These Tables list key protein targets and ligands in this article which are hyperlinked to corresponding entries in http://www.guidetopharmacology.org, the common portal for data from the IUPHAR/BPS Guide to PHARMACOLOGY (Southan *et al.*, 2016) and are permanently archived in the Concise Guide to PHARMACOLOGY 2015/16 (Alexander *et al.*, 2015a,b).

1. Introduction

Perivascular adipose tissue (PVAT) surrounds almost all blood vessels and is increasingly recognised as an important regulator of vascular tone. As an active endocrine organ the adipocytes and stromal cells within PVAT produce and secrete a range of adipokines, inflammatory cytokines, and other factors which can influence the tone of the underlying blood vessel (Dubrovska *et al.*, 2004; Malinowski *et al.*, 2008; Weston *et al.*, 2013). PVAT can release substances with vasodilatory activity such as adipocyte-derived relaxing factor (ADRF) (Galvez *et al.*, 2006; Lohn *et al.*, 2002; Verlohren *et al.*, 2004), leptin (Vecchione *et al.*, 2002), adiponectin (Chen *et al.*, 2003; Fesus *et al.*, 2007), angiotensin 1–7 (Ang 1-7) (Lee *et al.*, 2009), hydrogen peroxide (Gao *et al.*, 2007), nitric oxide (NO) (Gil-Ortega *et al.*, 2010) and hydrogen sulphide (H_2S) (Fang *et al.*, 2009) but also vasoconstrictor factors such as angiotensin II (Ang II) (Galvez-Prieto *et al.*, 2008) and superoxide anions (Gao *et al.*, 2006). Consequently, a balance exists and much research effort has been channeled into discovering what causes the function of PVAT to change in disease states such as obesity and metabolic syndrome where PVAT become deleterious to blood vessel activity.

PVAT is composed of brown adipocytes, white adipocytes or a mixture of both depending on the vascular bed (Cinti, 2011; Fitzgibbons *et al.*, 2011; Gao, 2007). In healthy humans and experimental animals, PVAT has a net anticontractile effect (Greenstein *et al.*, 2009; Lohn *et al.*, 2002), but the precise mechanisms remain elusive. The anti-contractile effect is likely due to release of transmissible factors; a process that requires calcium but is not dependent on perivascular nerve activity (Dubrovska *et al.*, 2004). In rat mesenteric vessels the anticontractile effect of PVAT is dependent on activation of delayed rectifier potassium channels (K_V) on the vascular smooth muscle (Verlohren *et al.*, 2004) while in rat aortic rings, Gao et al found that a PVAT-derived transmissible factor induced relaxation by: (1) an endothelium-dependent effect via NO release and subsequent K_{Ca} channel activation, and (2) an endothelium-independent mechanism involving H_2O_2 and subsequent activation of sGC (Gao *et al.*, 2007). More recent work has identified adiponectin as an abundant adipokine with anticontractile activity. In mouse mesenteric vessels and rat aorta, adiponectin was found to relax vascular smooth muscle cells via Kv channel opening and membrane hyperpolarisation (Fesus *et al.*, 2007). However, other studies using mouse mesenteric vessels found that adiponectin requires the presence of large conductance calcium-activated potassium channels (BK_{Ca}) in order to hyperpolarise VSMCs and exert an anticontractile effect (Lynch *et al.*, 2013). Interestingly, a recent study by Weston's group has shown that

adiponectin-mediated hyperpolarisation was inhibited by a selective inhibitor of AMP-activated protein kinase (AMPK) and that the effect of adiponectin was mimicked by the AMPK activator, A769662 (Weston *et al.*, 2013). Activation of AMPK is proposed to trigger opening of myocyte BK_{Ca} channels and release of NO which accounts for the anticontractile effect of adiponectin. Indeed, in mice lacking the AMPKα2 catalytic subunit isoform, globular adiponectin failed to induce vascular relaxation (Meijer *et al.*, 2013) suggesting that adiponectin requires AMPK to exert an anticontractile effect.

Although AMPK is often described as a cellular energy gauge and modulator of cellular metabolism (Hardie *et al.*, 2003), it also has important roles in maintaining vascular homeostasis (Ewart *et al.*, 2011). It is expressed throughout the vessel wall and can respond to changes in cellular energy state (Evans *et al.*, 2005; Fleming *et al.*, 2005), hormonal changes (Cheng *et al.*, 2007; Nagata *et al.*, 2004), and drugs (Bilodeau-Goeseels *et al.*, 2011; Ford *et al.*, 2012; Levine *et al.*, 2007) to regulate vascular tone. AMPK activation can induce vasodilation via phosphorylation and activation of endothelial NO synthase (eNOS) at Ser^{1177} (Davis *et al.*, 2006; Morrow *et al.*, 2003) and Ser^{633} (Chen *et al.*, 2009) to increase NO production and vascular relaxation (Davis *et al.*, 2006; Morrow *et al.*, 2003). AMPK can also induce endothelium-independent relaxation via reduced sensitivity of myosin light-chain kinase (MLCK) to intracellular calcium (Horman *et al.*, 2008). Collectively, these findings suggest that AMPK activation can induce vasodilation but may also be involved in the vascular effects of PVAT. However, despite AMPKα1 being the dominant vascular isoform, nothing is known about its role in mediating the anticontractile effect of PVAT.

The aim of this study was to investigate aortic PVAT function in a mouse with a global AMPKα1 isoform knockout. Furthermore, we wished to study whether lack of this AMPK isoform in the vascular wall affects the generation and vascular effects of adiponectin.

2. Methods

2.1. Animal model and artery preparation

Mice used in this study were housed at the University of Glasgow and maintained on 12 hour cycles of light and dark and at ambient temperature. Wild type (Sv129- WT) mice were originally purchased from Harlan Laboratories (Oxon, UK). AMPKα_1 knockout mice (KO) were kindly supplied by Benoit Viollet (Institut Cochin, Paris, France), the generation of which has been described previously (Jørgensen *et al.*, 2004). In all experiments age-matched male and female WT and KO mice were used since pilot experiments showed no gender difference in vessel contractility and relaxation (data not shown). Procedures conformed to the *Guide for the Care and Use of Laboratory Animals* published by the US National Institutes of Health (NIH Publication No. 85-23, revised 1996) and Directive 2010/63/EU of the European Parliament. Mice were terminally anaesthetized via intraperitoneal injection of sodium pentobarbital (200mg ml^{-1}) and the thoracic and abdominal aorta was removed to ice cold oxygenated (95% O_2:5% CO_2) Krebs' solution. In some experiments, mesenteric and other fat depots were also removed for histological analysis.

2.2. Histological analysis

Thoracic aortae with intact PVAT were fixed overnight in 10% acetic zinc formalin, dehydrated and embedded in paraffin. Sections (5 µm) of aorta were cut on a rotary microtome and stained with haematoxylin and eosin. To compare the morphology of aortic PVAT to other fat depots, mesenteric PVAT, subscapular brown adipose tissue (BAT) and epididymal white adipose tissue (WAT) were also fixed, sectioned and stained with H&E.

Immunohistochemistry was used to detect antigens of interest within the PVAT. Briefly, slides were deparaffinised and antigens were retrieved by heating in a microwave oven in Sodium Citrate buffer (10 mM Na citrate, 0.05% (v/v) Tween 20, pH 6.0) for 10 min. Slides were cooled at room temperature and endogenous peroxidase activity blocked by immersing in 3 % (v/v) H_2O_2 in methanol for 20 min. Non-specific antibody binding was blocked using 2.5 % (v/v) normal horse serum (ImmPRESS Reagent Kit, Vector labs, USA) for 1 h at room temperature and primary antibodies were then added overnight at 4^{o}C. Primary antibodies were diluted in 1 % (w/v) BSA in PBS and used at the following concentrations: anti-total AMPK 1:100 (Abcam #131512), anti-phospho-AMPK Thr172 1:100 (Cell Signalling Technology #2535), anti-UCP-1 1:500 (Abcam #10983). Blanks and negative controls were

included in each staining run. Secondary antibodies were incubated for 1 h at room temperature (ImmPRESS anti-rabbit Ig antibodies; Vector Labs, USA for UCP-1 or Biotinylated anti-rabbit IgG antibody from Histostain-Plus bulk kit, Life technologies, UK for total and phosphor-AMPK). Antibody binding was visualised using DAB (3,3' diaminobenzidine) chromogenic substrate (Vector Laboratories) and haematoxylin counter stain. Sections were photographed using AxioVision microscope software (Zeiss, Germany).

2.3. Small vessel wire myography

The thoracic and, in some experiments the abdominal aorta was cut into 2mm rings. Some rings were cleaned of PVAT and others were left with the PVAT intact. In all cases the endothelium on the luminal surface was removed by gently rubbing the interior of the vessel with a piece of fine wire and removal confirmed by lack of (<10%) vasodilator response to 10^{-6} M acetylcholine. Artery rings were mounted on two stainless steel pins in a four channel wire myograph (Danish Myo Technology), set to an optimum tension of 9.8 mN (Weingartner *et al.*, 2015) and allowed to equilibrate for at least 30 min before use. Vessels were bathed in Krebs' buffer of the following composition: 118 mM NaCl, 4.7 mM KCl, 1.2 mM $MgSO_4$, 25 mM $NaHCO_3$, 1.03 mM KH_2PO_4, 11 mM glucose and 2.5 mM $CaCl_2$ at 37ºC and gassed continuously with 95% O_2 and 5% CO_2. Reproducible responses were obtained to 40mM KCl and 30nM 9,11-Dideoxy-9α,11α-methanoepoxy prostaglandin $F_{2\alpha}$ (U46619, Tocris) before commencing experiments. Cumulative concentration-response curves to the K^+ channel opener cromakalim ($1x10^{-9}$ to $1x10^{-6}$ M; Sigma-Aldrich, Poole, UK), added at 10 min intervals were constructed. Data were expressed as a percentage loss of U46619-induced tone.

To produce conditioned media (CM), thoracic aortic PVAT from WT and KO mice was carefully dissected, weighed and incubated in warmed Krebs' solution at 37 ˚C for 1 h. The conditioned medium was transferred to the recipient myograph chamber containing an aortic ring at baseline tension. The ring was then contracted and dose-response curves to cromakalim constructed as previously. In some experiments, PVAT from KO mice was added to WT aortic rings and vice-versa (termed a cross-over experiment).

To study the role of adiponectin in the anticontractile effect of PVAT, two separate experiments were performed. Firstly, 5µg mL^{-1} of an adiponectin blocking peptide against adiponectin receptor 1 (AdipoR1; GeneTex, UK) was added to preconstricted aortic rings

with and without PVAT. Secondly, globular adiponectin (1µg mL^{-1} diluted in 1% (w/v) bovine serum albumin (BSA); Enzo Life Sciences Ltd, UK) was added to arteries prior to contracting with U46619. In both cases, dose-response curves to cromakalim were then constructed in WT and KO aortic rings.

2.4. Effect of cromakalim on AMPK activity in cultured cells

Rat aortic smooth muscle cells from Wistar-Kyoto rats were provided Dr Augusto Montezano (University of Glasgow) and maintained in Dulbecco's modified Eagle medium (DMEM) supplemented with 10% (v/v) FBS (Invitrogen, UK), 100 U ml^{-1} pencillin and 100 µg ml^{-1} streptomycin. At passage 4 to 5 the cells were washed with PBS and incubated in serum-free medium for 2 hours. Cells were incubated with the AMPK-activating agent AICAR (10^{-2}-10^{-3}M) or cromakalim (10^{-8}-10^{-6}M) for 45 minutes, the medium was removed, lysis buffer added (50 mM Tris pH7.4, 50 mM NaF, 1 mM $Na_4P_2O_7$, 1 mM EGTA, 1mM EDTA, 1% (v/v) Triton X-100, 1 mM DTT and 1% cocktail of protease inhibitors with 2mM Na_3VO_4) and the cells collected by scraping. Lysates were placed on ice for 30 min, centrifuged at 8000 rpm for 10 min and supernatants collected and used for immunoblotting.

2.5 Protein expression/immunoblotting

The protein content of VSMC lysates (or in some experiments PVAT lysates or conditioned media samples) was determined using Coomassie Plus Protein Assay Reagent (Perbio, USA) against a BSA standard curve. Samples were run on NuPAGE Novex 4-12 % Bis-Tris mini gels (Life Technologies), transferred to nitrocellulose membranes and incubated with specific rabbit anti-total AMPKα (Cell Signalling Technology #2603), anti-AMPKα1(Abcam #ab110036), anti-AMPKα2 (Generous gift from Prof. Grahame Hardie, University of Dundee, UK), anti-phospho-Thr^{172} AMPK (Cell Signalling Technology #2535) and anti-phospho-Ser^{79} ACC (Cell Signalling Technology #3661) antibodies. All primary antibodies were diluted 1:1000 in 50% (v/v) TBS, 50% (v/v) Odyssey®-Block (LI-COR, USA). Immunolabelled proteins were visualized using infrared dye-labelled secondary antibodies and an Odyssey Sa Infrared Imaging System (LI-COR, USA) and expression normalised to anti-GAPDH antibody immunoreactivity (Cell Signaling Technology).

2.6 Array and adiponectin ELISA

Adipokine expression profiling was performed using an Adipokine proteome profiler, (R&D systems, UK) following the protocol provided by the manufacturer. Briefly, 1 ml of pooled samples of homogenised PVAT or conditioned medium from WT and KO mice were added to the array membranes and incubated at 4°C overnight. After washing, membranes were incubated with 2 ml of horseradish peroxidase–conjugated streptavidin at room temperature for 30 min and the presence of adipokines detected by chemiluminescence. The resultant film images were scanned with a densitometer and converted to densitometric units using Quantity One software (Bio-Rad Laboratories, Hercules, CA, USA). Data were normalized against an internal control as recommended by the manufacturer.

To study adiponectin release by PVAT, a mouse adiponectin/Acrp30 Quantikine ELISA Kit (MRP300, R&D systems, Minneapolis, MN) was used. Samples of homogenised PVAT and conditioned media from WT and KO mice were prepared and protein concentration determined. Adiponectin was detected as a colourimetric reaction measuring absorbance of the ELISA plate at 450 nm with wavelength correction using a FLUOstar OPTIMA microplate reader (BMG Labtech, Germany). The mean absorbance from each sample was measured in duplicate and the adiponectin concentration was determined by comparison with the standard curve.

2.7. Statistical analysis

All results are expressed as mean ± standard error of the mean (SEM). The n number stated in all cases represents the number of mice from which tissue was obtained. Data were analysed with GraphPad Prism 5.0 software. Myography data was analysed using 2-way ANOVA. When comparing three or more data groups, two-way ANOVA followed by Bonferroni post-hoc tests were used. When comparing two or more data groups a Newman–Keuls post hoc test was used. In all cases, a p value of less than 0.05 was considered statistically significant.

3. Results

3.1. PVAT morphology and AMPK expression

In haematoxylin and eosin stained sections, there were no gross differences in PVAT or other fat depots between WT and AMPKα_1 KO mice (Figure 1). In both strains, thoracic PVAT had the appearance of BAT with round nuclei, and small, multilocular lipid droplets, whereas mesenteric PVAT was very similar to WAT, with large single lipid vacuoles and marginal nuclei. Abdominal PVAT showed features of both BAT and WAT. Immunohistochemical staining for the brown adipose tissue marker UCP-1 was similar in WT and KO aortic PVAT with very low staining in mesenteric fat and some staining present in abdominal aortic PVAT (supplementary Figure S1, S2).

AMPKα and phospho-AMPKα (pAMPKα) were detected immunohistochemically in thoracic PVAT and there was a marked reduction in both total and phospho-AMPKα Thr172 in KO mice (data not shown). Western blotting was used to quantify AMPK levels in homogenised PVAT. As expected, there was a marked reduction in total levels of AMPKα, phospho-AMPKα Thr^{172} and phospho-ACC Ser^{79} (pACC). When expressed relative to total AMPKα, there was a modest reduction in the level of phosphorylated AMPKα in KO mice in comparison with wild type (Figure 2). There was no substantial difference in AMPKα2 immunoreactivity between genotypes.

3.2. Anticontractile effect of PVAT and importance of AMPK

The presence or absence of the vascular endothelium did not affect the contractile response to U46619 in WT or KO aortae (data not shown). In aortic rings without PVAT there was no significant difference in contraction between WT and KO mice (Figure 3A). In rings containing PVAT, contraction to U46619 was significantly reduced in the WT but not the KO mice (Figure 3A), indicating an anticontractile effect of the PVAT which was lost when the PVAT is deficient in AMPKα1.

The presence of PVAT significantly increased the relaxation to cromakalim in thoracic aortic rings from WT mice but this effect was completely absent in AMPKα1 KO mice (Figure 3B, C). To check that the effect of PVAT was not specific to the thoracic aorta, the experiment was repeated in abdominal aorta and similar results were found: WT vessels with intact PVAT, maximum relaxation (E_{max}) to cromakalim was 53.3 ± 5.2% with PVAT, and 24.5 ±

5.7% without PVAT (n = 6; $p<0.05$ vs. PVAT+) while in KO mice PVAT had no effect on E_{max} to cromakalim (22.8 ± 5.8% vs. 17.4 ± 4.1%, n = 6; p=ns).

In WT mice, PVAT which had been dissected free of the artery and added back into the organ bath was able to augment relaxation to cromakalim equally as well as when the PVAT was in contact with the artery (E_{max} 54.5± 8.3% vs. 49.9 ± 6.7%; n=5; p=ns), suggesting the PVAT releases a transmissible factor which is responsible for increased relaxation. In contrast, addition of PVAT from KO mice to an aortic ring from WT mice did not augment relaxation to cromakalim (Figure 4A, B) whereas adding WT PVAT to a KO aortic ring did augment relaxation. Furthermore, addition of conditioned media (CM) produced by WT PVAT was able to augment cromakalim-induced relaxation in WT aortic rings while CM produced by KO PVAT was unable to augment relaxation (Figure 4C, D). Wild type CM also significantly attenuated contraction to U46619 in WT rings without PVAT (1.19 ± 0.1g vs. 0.86 ± 0.1 g with addition of CM; n=12; $p<0.05$). In contrast, KO conditioned media showed a non-significant trend toward increased contraction (2.33 ± 1.3g vs. 2.80 ± 1.4g with addition of CM; n =12). Transfer of WT PVAT into KO vessels without PVAT and CM experiments indicates that the deficiency in the KO mouse is likely to be at least partly related to differences in release of adipokines by the PVAT.

3.3. Cromakalim does not activate AMPK in vascular smooth muscle cells

To rule out the possibility that vasodilation to cromakalim is altered in KO mice because cromakalim activates AMPK, cultured rat VSMCs were treated with a range of concentrations of cromakalim and the AMPK activator AICAR as a positive control. Cromakalim did not increase phosphorylation of AMPK in the vascular smooth muscle and had no effect on the phosphorylation of the downstream substrate ACC. AICAR caused an increase in AMPK activity (supplementary Figure S3) at a concentration of 10^{-3} M.

3.4 Adipocytokine profile and effect of AMPK KO

Adipocytokine profiling of PVAT-derived conditioned media showed a striking reduction in the amount of adiponectin released by PVAT from AMPKα1 KO mice (n=2; data not shown). Further quantification of this difference by ELISA in n=5 samples of conditioned medium from KO and WT mice revealed a significant reduction in the quantity of adiponectin released by KO PVAT (Figure 5).

3.5 Effect on adiponectin on vessel function

Addition of globular adiponectin to WT aortic rings without PVAT significantly increased relaxation to cromakalim (Figure 6A). Interestingly, globular adiponectin enhanced the relaxation to cromakalim in KO vessels both with and without PVAT (Figure 6B, C). Blocking adiponectin receptors in WT aortic rings with intact PVAT significantly attenuated relaxation to cromakalim (Figure 7A) while in KO arteries with intact PVAT, the blocking peptide had no effect (Figure 7B). Taken together, these results suggest that KO PVAT releases less adiponectin but that the medial smooth muscle cells are still able to respond to exogenously added adiponectin.

4. Discussion

The main findings of this study are that the anticontractile effect of aortic PVAT is lost in mice which lack AMPKα1 and this is due to reduced generation of a transmissible factor, likely adiponectin, by the PVAT. The results also demonstrate that the lack of an anticontractile effect in the KO mouse is not due to alterations in PVAT morphology or the ratio of BAT to WAT or to the absence of AMPK expression in the medial smooth muscle cells of the aorta. Since incubation with globular adiponectin augmented relaxation to cromakalim in KO arteries without PVAT, it is also unlikely to be due to a reduced sensitivity of the medial VSMCs to adiponectin. In summary, AMPKα1 plays a critical role in maintaining the anticontractile actions of PVAT; an effect independent of the endothelium but likely mediated through altered adiponectin secretion.

Morphological studies revealed no difference in PVAT from WT and KO mice. Thoracic aorta was similar in appearance to depots of BAT from the subscapsular region while abdominal aorta showed a mixture of WAT and BAT. This is in agreement with previous studies using Sv129 mice (Cinti, 2011; Frontini *et al.*, 2010) and also from other mouse strains (Cannon *et al.*, 2004; Fitzgibbons *et al.*, 2011; Padilla *et al.*, 2013). It has been speculated that differences in PVAT phenotype could contribute to disease susceptibility of certain regions of the arterial tree (Greif *et al.*, 2009; Jeong *et al.*, 2007), possibly through release of proinflammatory cytokines (Chatterjee *et al.*, 2009; Payne *et al.*, 2010; Zhao *et al.*, 2003). Certainly, in animal models of obesity, there is evidence for a detrimental effect of PVAT on vascular function in aortic (Ma *et al.*, 2010) and mesenteric arteries (Ketonen *et al.*, 2010; Marchesi *et al.*, 2009) and in animals fed a high fat diet, there was reduced phosphorylation of AMPK in thoracic aortic PVAT, an increased adipocyte size and increased intimal thickness (Ma *et al.*, 2010). Taken together, these studies suggest that AMPK in the PVAT is likely to be protective and this agrees with the data presented here showing that the anticontractile effect of thoracic (and abdominal) PVAT is lost in mice lacking AMPKα1. We also demonstrated that in the KO mouse there was reduced phosphorylated and total AMPK in PVAT as well as reduced phosphorylation of the downstream kinase ACC. There was also no obvious compensatory upregulation in AMPKα2 isoforms. The dramatic effect of α1 KO on PVAT function is in agreement with other studies showing that in adipose tissue the catalytic α_1 subunit is the major isoform expressed and is also responsible for the major part of AMPK activity (Daval *et al.*, 2005; Lihn *et al.*, 2004).

The lack of AMPKα1 caused the PVAT to lose its anticontractile effect and its presence no longer augmented relaxation to cromakalim. To rule out any differences being due to cromakalim acting through AMPK, we added cromakalim to cultured vascular smooth muscle cells and found it had no effect on AMPK expression or phosphorylation. Many other studies have found an anticontractile effect of PVAT in a variety of vascular beds (Gao *et al.*, 2005b; Greenstein *et al.*, 2009) and in vessels contracted with several different vasoconstrictor agents including phenylephrine, 5-HT, angiotensin II and U 46619 (Gao *et al.*, 2005a; Lohn *et al.*, 2002; Verlohren *et al.*, 2004). The mechanism has been proposed as release of transferable relaxation factor(s), termed adventitia-derived relaxation factor (ADRF). The nature of ADRF is largely unknown. However, it has been shown to act in part via activation of K^+ channels and tyrosine kinase and independent of NO and sympathetic nerve stimulation (Lohn *et al.*, 2002). Our data agree with this in that transfer of CM from WT mice augmented relaxation of aortic rings with PVAT. In addition, it was not necessary for the PVAT to be in contact with the vessel to exert an anticontractile effect. In our protocol we added the CM prior to contraction of the vessel ring with U46619 and found that WT but not KO CM attenuated aortic contraction. This strongly suggests a transmissible factor is responsible for attenuating contraction and augmenting relaxation which is produced by aortic PVAT and in the KO mice this factor is reduced or absent. The deficiency in the KO mouse is unlikely to be due to a lack of AMPK in the medial smooth muscle cells since in cross over studies WT PVAT was able to augment the relaxation response to cromakalim in KO vessels. However, it is worth noting that relaxations to cromakalim tended to be lower in KO rings without PVAT and while exogenously added WT PVAT or WT conditioned media significantly augmented relaxation to cromakalim in KO aortic rings, it still did not reach levels seen in WT vessels with intact PVAT. This suggests there may be some deficit in function of the VSMCs in the KO mice and future experiments should use an adipocyte-specific AMPK KO to address this.

The release of the vasorelaxing factors (ADRF) has been reported to be dependent on calcium (Ca^{2+}) and is regulated by intracellular signalling pathways involving tyrosine kinase and protein kinase A and not to be dependent on perivascular nerve endings (Dubrovska *et al.*, 2004). There are very few studies where the role of AMPK in release of ADRFs has been investigated. A study by Lihn *et al* indicated that the AMPK activator AICAR stimulated adipose tissue AMPKα1 activity and adiponectin gene expression and reduced the release of TNF-α and IL-6 (Lihn *et al.*, 2004). These cytokines have been shown to have inhibitory

effects on adiponectin gene expression and release (Fasshauer *et al.*, 2002; Lihn *et al.*, 2003; Maeda *et al.*, 2002), meaning that activity of AMPK in the PVAT could regulate adiponectin expression (Lihn *et al.*, 2004). Similarly, the PPARγ agonist troglitazone which also activates AMPK has a positive effect on adiponectin expression in mature adipocytes (Phillips *et al.*, 2003). However, other studies using cultured 3T3-L1 adipocytes found that prolonged exposure to AMPK activating agents actually causes a significant reduction in adiponectin protein content of the adipocytes (Huypens *et al.*, 2005).

To clarify how AMPKα1 KO affects the secretion of adipocytokines by aortic PVAT, we performed an array and the most striking difference was a reduction in adiponectin in KO PVAT and CM. Quantitative studies using ELISA further confirmed a significant reduction in adiponectin in KO CM. Since adiponectin is a vasodilator (Fesus *et al.*, 2007), it could account for the lack of an anticontractile effect in KO PVAT. Indeed, in WT mice the anticontractile effect of PVAT was abolished using a adiponectin receptor blocking peptide, an effect demonstrated previously in human gluteal arteries (Fesus *et al.*, 2007) and mouse mesenteric arteries (Lynch *et al.*, 2013). We also demonstrated the ability of both KO and WT aortic rings without PVAT to increase relaxation to cromakalim when pretreated with globular adiponectin. Since all rings were denuded of endothelium, it suggests the ability of adiponectin having direct access to vascular smooth muscle cells (Weston *et al.*, 2013). The adiponectin enhanced vascular relaxation was also observed in in KO vessels with intact PVAT, indicating that there was no perfusion barrier between PVAT and vascular smooth muscle layer. Additionally, vascular relaxation was seen in both wild type and AMPKα1 knockout vessels suggesting that adiponectin can act directly on vascular smooth muscle cells and that the AMPKα1 isoform is not involved.

Only one vasodilator was used in the current study; the K_{ATP} channel activator cromakalim. K_{ATP} channels in VSMCs may be involved in mediating the anticontractile effects of PVAT since a previous study showed an inhibitory effect of glibenclamide (Lohn *et al.*, 2002). K_{ATP} channels appear to regulate basal tone in a number of vascular bed such as coronary circulation (Samaha *et al.*, 1992) and mesenteric vessels (Nelson *et al.*, 1995) and inhibition of this channel by glibenclamide has been found to attenuate coronary and cerebral autoregulation (Hong *et al.*, 1994; Narishige *et al.*, 1993). In our study, since PVAT enhanced the relaxation induced by cromakalim, adiponectin released by the PVAT may act in part through modulating K_{ATP} channels. However, the role and the mechanism of activation need to be further investigated.

In conclusion, we have shown that PVAT has a profound anticontractile effect on mouse aortic rings. The effect may be due to release of adiponectin by the PVAT and this release is regulated by the activity of AMPKα1. In mouse aortic rings, adiponectin augments relaxation to cromakalim in an endothelium-independent manner although other effects of adiponectin on the endothelium cannot be ruled out. Indeed, although aortic rings in this study were mechanically denuded, endothelial cells in vessels within the vasa vasorum will remain and adiponectin may have effects here. Clinically, there is evidence that PVAT becomes dysfunctional in obese humans and plasma adiponectin is reduced (Aghamohammadzadeh *et al.*, 2015). Alterations in AMPK activity in the PVAT may be behind this effect.

Conflicts of interest:

There are no conflicts of interest to declare

Author contributions:

TAM, ABU & OJK performed the experiments, acquired and analysed the data and prepared the figures. TAM drafted sections of the paper. IS & SK conceived and planned the experiments, SK prepared the final version of the manuscript and SK and IS proof read the final version of manuscript.

References:

Aghamohammadzadeh R, Unwin RD, Greenstein AS, Heagerty AM (2015). Effects of Obesity on Perivascular Adipose Tissue Vasorelaxant Function: Nitric Oxide, Inflammation and Elevated Systemic Blood Pressure. *J Vasc Res* **52**(5)**:** 299-305.

Alexander SP, Kelly E, Marrion N, Peters JA, Benson HE, Faccenda E, Pawson AJ, Sharman JL, Southan C, Buneman OP, Catterall WA, Cidlowski JA, Davenport AP, Fabbro D, Fan G, McGrath JC, Spedding M, Davies JA (2015). CGTP Collaborators. The Concise Guide to PHARMACOLOGY 2015/16: Overview. *Br J Pharmacol.* **172**(24): 5729-5743.

Bilodeau-Goeseels S, Panich PL, Kastelic JP (2011). Activation of AMP-activated protein kinase may not be involved in AICAR- and metformin-mediated meiotic arrest in bovine denuded and cumulus-enclosed oocytes in vitro. *Zygote* **19**(2)**:** 97-106.

Cannon B, Nedergaard J (2004). Brown adipose tissue: function and physiological significance. *Physiol Rev* **84**(1)**:** 277-359.

Chatterjee TK, Stoll LL, Denning GM, Harrelson A, Blomkalns AL, Idelman G, *et al.* (2009). Proinflammatory phenotype of perivascular adipocytes: influence of high-fat feeding. *Circ Res* **104**(4)**:** 541-549.

Chen H, Montagnani M, Funahashi T, Shimomura I, Quon MJ (2003). Adiponectin Stimulates Production of Nitric Oxide in Vascular Endothelial Cells. *Journal of Biological Chemistry* **278**(45)**:** 45021-45026.

Chen Z, Peng IC, Sun W, Su MI, Hsu PH, Fu Y, *et al.* (2009). AMP-activated protein kinase functionally phosphorylates endothelial nitric oxide synthase Ser633. *Circ Res* **104**(4)**:** 496-505.

Cheng KK, Lam KS, Wang Y, Huang Y, Carling D, Wu D, *et al.* (2007). Adiponectin-induced endothelial nitric oxide synthase activation and nitric oxide production are mediated by APPL1 in endothelial cells. *Diabetes* **56**(5)**:** 1387-1394.

Cinti S (2011). Between brown and white: novel aspects of adipocyte differentiation. *Ann Med* **43**(2)**:** 104-115.

Daval M, Diot-Dupuy F, Bazin R, Hainault I, Viollet B, Vaulont S, *et al.* (2005). Anti-lipolytic action of AMP-activated protein kinase in rodent adipocytes. *J Biol Chem* **280**(26)**:** 25250-25257.

Davis BJ, Xie Z, Viollet B, Zou MH (2006). Activation of the AMP-activated kinase by antidiabetes drug metformin stimulates nitric oxide synthesis in vivo by promoting the association of heat shock protein 90 and endothelial nitric oxide synthase. *Diabetes* **55**(2)**:** 496-505.

Dubrovska G, Verlohren S, Luft FC, Gollasch M (2004). Mechanisms of ADRF release from rat aortic adventitial adipose tissue. *Am J Physiol Heart Circ Physiol* **286**(3)**:** H1107-1113.

Evans AM, Mustard KJ, Wyatt CN, Peers C, Dipp M, Kumar P, *et al.* (2005). Does AMP-activated protein kinase couple inhibition of mitochondrial oxidative phosphorylation by hypoxia to calcium signaling in O2-sensing cells? *J Biol Chem* **280**(50)**:** 41504-41511.

Ewart MA, Kennedy S (2011). AMPK and vasculoprotection. *Pharmacol Ther* **131**(2)**:** 242-253.

Fang L, Zhao J, Chen Y, Ma T, Xu G, Tang C, *et al.* (2009). Hydrogen sulfide derived from periadventitial adipose tissue is a vasodilator. *J Hypertens* **27**(11)**:** 2174-2185.

Fasshauer M, Klein J, Neumann S, Eszlinger M, Paschke R (2002). Hormonal regulation of adiponectin gene expression in 3T3-L1 adipocytes. *Biochem Biophys Res Commun* **290**(3)**:** 1084-1089.

Fesus G, Dubrovska G, Gorzelniak K, Kluge R, Huang Y, Luft FC, *et al.* (2007). Adiponectin is a novel humoral vasodilator. *Cardiovasc Res* **75**(4)**:** 719-727.

Fitzgibbons TP, Kogan S, Aouadi M, Hendricks GM, Straubhaar J, Czech MP (2011). Similarity of mouse perivascular and brown adipose tissues and their resistance to diet-induced inflammation. *Am J Physiol-Heart C* **301**(4)**:** H1425-H1437.

Fleming I, Fisslthaler B, Dixit M, Busse R (2005). Role of PECAM-1 in the shear-stress-induced activation of Akt and the endothelial nitric oxide synthase (eNOS) in endothelial cells. *J Cell Sci* **118**(Pt 18)**:** 4103-4111.

Ford RJ, Teschke SR, Reid EB, Durham KK, Kroetsch JT, Rush JW (2012). AMP-activated protein kinase activator AICAR acutely lowers blood pressure and relaxes isolated resistance arteries of hypertensive rats. *J Hypertens* **30**(4)**:** 725-733.

Frontini A, Cinti S (2010). Distribution and development of brown adipocytes in the murine and human adipose organ. *Cell Metab* **11**(4)**:** 253-256.

Galvez-Prieto B, Bolbrinker J, Stucchi P, de Las Heras AI, Merino B, Arribas S, *et al.* (2008). Comparative expression analysis of the renin-angiotensin system components between white and brown perivascular adipose tissue. *J Endocrinol* **197**(1)**:** 55-64.

Galvez B, de Castro J, Herold D, Dubrovska G, Arribas S, Gonzalez MC, *et al.* (2006). Perivascular adipose tissue and mesenteric vascular function in spontaneously hypertensive rats. *Arterioscler Thromb Vasc Biol* **26**(6)**:** 1297-1302.

Gao YJ (2007). Dual modulation of vascular function by perivascular adipose tissue and its potential correlation with adiposity/lipoatrophy-related vascular dysfunction. *Curr Pharm Des* **13**(21)**:** 2185-2192.

Gao YJ, Holloway AC, Zeng ZH, Lim GE, Petrik JJ, Foster WG, *et al.* (2005a). Prenatal exposure to nicotine causes postnatal obesity and altered perivascular adipose tissue function. *Obes Res* **13**(4)**:** 687-692.

Gao YJ, Lu C, Su LY, Sharma AM, Lee RM (2007). Modulation of vascular function by perivascular adipose tissue: the role of endothelium and hydrogen peroxide. *Br J Pharmacol* **151**(3)**:** 323-331.

Gao YJ, Takemori K, Su LY, An WS, Lu C, Sharma AM, *et al.* (2006). Perivascular adipose tissue promotes vasoconstriction: the role of superoxide anion. *Cardiovasc Res* **71**(2)**:** 363-373.

Gao YJ, Zeng ZH, Teoh K, Sharma AM, Abouzahr L, Cybulsky I, *et al.* (2005b). Perivascular adipose tissue modulates vascular function in the human internal thoracic artery. *J Thorac Cardiovasc Surg* **130**(4)**:** 1130-1136.

Gil-Ortega M, Stucchi P, Guzman-Ruiz R, Cano V, Arribas S, Gonzalez MC, *et al.* (2010). Adaptative nitric oxide overproduction in perivascular adipose tissue during early diet-induced obesity. *Endocrinology* **151**(7)**:** 3299-3306.

Greenstein AS, Khavandi K, Withers SB, Sonoyama K, Clancy O, Jeziorska M, *et al.* (2009). Local inflammation and hypoxia abolish the protective anticontractile properties of perivascular fat in obese patients. *Circulation* **119**(12)**:** 1661-1670.

Greif M, Becker A, von Ziegler F, Lebherz C, Lehrke M, Broedl UC, *et al.* (2009). Pericardial Adipose Tissue Determined by Dual Source CT Is a Risk Factor for Coronary Atherosclerosis. *Arteriosclerosis, Thrombosis, and Vascular Biology* **29**(5)**:** 781-786.

Hardie DG, Scott JW, Pan DA, Hudson ER (2003). Management of cellular energy by the AMP-activated protein kinase system. *FEBS Lett* **546**(1)**:** 113-120.

Hong KW, Pyo KM, Lee WS, Yu SS, Rhim BY (1994). Pharmacological evidence that calcitonin gene-related peptide is implicated in cerebral autoregulation. *American Journal of Physiology - Heart and Circulatory Physiology* **266**(1)**:** H11-H16.

Horman S, Morel N, Vertommen D, Hussain N, Neumann D, Beauloye C, *et al.* (2008). AMP-activated protein kinase phosphorylates and desensitizes smooth muscle myosin light chain kinase. *J Biol Chem* **283**(27)**:** 18505-18512.

Huypens P, Quartier E, Pipeleers D, Van de Casteele M (2005). Metformin reduces adiponectin protein expression and release in 3T3-L1 adipocytes involving activation of AMP activated protein kinase. *European Journal of Pharmacology* **518**(2–3)**:** 90-95.

Jeong JW, Jeong MH, Yun KH, Oh SK, Park EM, Kim YK, *et al.* (2007). Echocardiographic epicardial fat thickness and coronary artery disease. *Circulation Journal* **71**(4)**:** 536-539.

Jørgensen SB, Viollet B, Andreelli F, Frøsig C, Birk JB, Schjerling P, *et al.* (2004). Knockout of the α2 but Not α1 5′-AMP-activated Protein Kinase Isoform Abolishes 5-Aminoimidazole-4-carboxamide-1-β-4-ribofuranosidebut Not Contraction-induced Glucose Uptake in Skeletal Muscle. *Journal of Biological Chemistry* **279**(2)**:** 1070-1079.

Ketonen J, Shi J, Martonen E, Mervaala E (2010). Periadventitial adipose tissue promotes endothelial dysfunction via oxidative stress in diet-induced obese C57Bl/6 mice. *Circ J* **74**(7)**:** 1479-1487.

Lee RM, Lu C, Su LY, Gao YJ (2009). Endothelium-dependent relaxation factor released by perivascular adipose tissue. *J Hypertens* **27**(4)**:** 782-790.

Levine YC, Li GK, Michel T (2007). Agonist-modulated regulation of AMP-activated protein kinase (AMPK) in endothelial cells. Evidence for an AMPK -> Rac1 -> Akt -> endothelial nitric-oxide synthase pathway. *J Biol Chem* **282**(28)**:** 20351-20364.

Lihn AS, Jessen N, Pedersen SB, Lund S, Richelsen B (2004). AICAR stimulates adiponectin and inhibits cytokines in adipose tissue. *Biochem Biophys Res Commun* **316**(3)**:** 853-858.

Lihn AS, Richelsen B, Pedersen SB, Haugaard SB, Rathje GS, Madsbad S, *et al.* (2003). Increased expression of TNF-alpha, IL-6, and IL-8 in HALS: implications for reduced adiponectin expression and plasma levels. *Am J Physiol Endocrinol Metab* **285**(5)**:** E1072-1080.

Lohn M, Dubrovska G, Lauterbach B, Luft FC, Gollasch M, Sharma AM (2002). Periadventitial fat releases a vascular relaxing factor. *FASEB J* **16**(9)**:** 1057-1063.

Lynch FM, Withers SB, Yao Z, Werner ME, Edwards G, Weston AH, *et al.* (2013). Perivascular adipose tissue-derived adiponectin activates BK(Ca) channels to induce anticontractile responses. *Am J Physiol Heart Circ Physiol* **304**(6)**:** H786-795.

Ma L, Ma S, He H, Yang D, Chen X, Luo Z, *et al.* (2010). Perivascular fat-mediated vascular dysfunction and remodeling through the AMPK/mTOR pathway in high-fat diet-induced obese rats. *Hypertens Res* **33**(5)**:** 446-453.

Maeda N, Shimomura I, Kishida K, Nishizawa H, Matsuda M, Nagaretani H, *et al.* (2002). Diet-induced insulin resistance in mice lacking adiponectin/ACRP30. *Nat Med* **8**(7)**:** 731-737.

Malinowski M, Deja MA, Golba KS, Roleder T, Biernat J, Wos S (2008). Perivascular tissue of internal thoracic artery releases potent nitric oxide and prostacyclin-independent anticontractile factor. *Eur J Cardiothorac Surg* **33**(2)**:** 225-231.

Marchesi C, Ebrahimian T, Angulo O, Paradis P, Schiffrin EL (2009). Endothelial nitric oxide synthase uncoupling and perivascular adipose oxidative stress and inflammation contribute to vascular dysfunction in a rodent model of metabolic syndrome. *Hypertension* **54**(6)**:** 1384-1392.

Meijer RI, Bakker W, Alta CL, Sipkema P, Yudkin JS, Viollet B, *et al.* (2013). Perivascular adipose tissue control of insulin-induced vasoreactivity in muscle is impaired in db/db mice. *Diabetes* **62**(2)**:** 590-598.

Morrow VA, Foufelle F, Connell JM, Petrie JR, Gould GW, Salt IP (2003). Direct activation of AMP-activated protein kinase stimulates nitric-oxide synthesis in human aortic endothelial cells. *J Biol Chem* **278**(34)**:** 31629-31639.

Nagata D, Takeda R, Sata M, Satonaka H, Suzuki E, Nagano T, *et al.* (2004). AMP-activated protein kinase inhibits angiotensin II-stimulated vascular smooth muscle cell proliferation. *Circulation* **110**(4)**:** 444-451.

Narishige T, Egashira K, Akatsuka Y, Katsuda Y, Numaguchi K, Sakata M, *et al.* (1993). Glibenclamide, a putative ATP-sensitive K+ channel blocker, inhibits coronary autoregulation in anesthetized dogs. *Circ Res* **73**(4)**:** 771-776.

Nelson MT, Quayle JM (1995). Physiological roles and properties of potassium channels in arterial smooth muscle. *Am J Physiol* **268**(4 Pt 1)**:** C799-822.

Padilla J, Jenkins NT, Vieira-Potter VJ, Laughlin MH (2013). Divergent phenotype of rat thoracic and abdominal perivascular adipose tissues. *Am J Physiol Regul Integr Comp Physiol* **304**(7)**:** R543-552.

Payne GA, Borbouse L, Kumar S, Neeb Z, Alloosh M, Sturek M, *et al.* (2010). Epicardial Perivascular Adipose-Derived Leptin Exacerbates Coronary Endothelial Dysfunction in Metabolic Syndrome via a Protein Kinase C-β Pathway. *Arteriosclerosis, Thrombosis, and Vascular Biology* **30**(9)**:** 1711-1717.

Phillips SA, Ciaraldi TP, Kong AP, Bandukwala R, Aroda V, Carter L, *et al.* (2003). Modulation of circulating and adipose tissue adiponectin levels by antidiabetic therapy. *Diabetes* **52**(3)**:** 667-674.

Samaha FF, Heineman FW, Ince C, Fleming J, Balaban RS (1992). ATP-sensitive potassium channel is essential to maintain basal coronary vascular tone in vivo. *American Journal of Physiology - Cell Physiology* **262**(5)**:** C1220-C1227.

Southan C, Sharman JL, Benson HE, Faccenda E, Pawson AJ, Alexander SP, Buneman OP, Davenport AP, McGrath JC, Peters JA, Spedding M, Catterall WA, Fabbro D, Davies JA (2015) NC-IUPHAR. The IUPHAR/BPS Guide to PHARMACOLOGY in 2016: towards curated quantitative interactions between 1300 protein targets and 6000 ligands. *Nucleic Acids Res.* **44**(D1): D1054-1068.

Vecchione C, Maffei A, Colella S, Aretini A, Poulet R, Frati G, *et al.* (2002). Leptin effect on endothelial nitric oxide is mediated through Akt-endothelial nitric oxide synthase phosphorylation pathway. *Diabetes* **51**(1)**:** 168-173.

Verlohren S, Dubrovska G, Tsang SY, Essin K, Luft FC, Huang Y, *et al.* (2004). Visceral periadventitial adipose tissue regulates arterial tone of mesenteric arteries. *Hypertension* **44**(3)**:** 271-276.

Weingartner O, Husche C, Schott HF, Speer T, Bohm M, Miller CM, *et al.* (2015). Vascular effects of oxysterols and oxyphytosterols in apoE -/- mice. *Atherosclerosis* **240**(1)**:** 73-79.

Weston AH, Egner I, Dong Y, Porter EL, Heagerty AM, Edwards G (2013). Stimulated release of a hyperpolarizing factor (ADHF) from mesenteric artery perivascular adipose tissue: involvement of myocyte BKCa channels and adiponectin. *Br J Pharmacol* **169**(7)**:** 1500-1509.

Zhao H, Kalivendi S, Zhang H, Joseph J, Nithipatikom K, Vásquez-Vivar J, *et al.* (2003). Superoxide reacts with hydroethidine but forms a fluorescent product that is distinctly different from ethidium: potential implications in intracellular fluorescence detection of superoxide. *Free Radical Biology and Medicine* **34**(11)**:** 1359-1368.

Figure & Legends:

Figure 1: Representative photomicrographs showing the morphology of fat depots in WT and AMPKα1 KO mice. Panels A & B- subscapular brown adipose tissue (BAT) Panels C & D- epididymal white adipose tissue (WAT), Panels E & F- thoracic perivascular adipose tissue (PVAT), Panels G & H- abdominal PVAT and Panels I & J- mesenteric PVAT. Aortic PVAT had the morphology of BAT. AO= aorta, MA= mesenteric artery, scale bar = 20μm).

Figure 2: Western blotting showing expression of AMPKα isoforms and the downstream kinase ACC expression in PVAT from WT (right lanes) and KO mice (left lanes). KO mouse PVAT showed a reduction in expression of AMPKα1 and total AMPKα with no change in AMPKα2. KO PVAT also had significantly reduced phosphoAMPK and ACC. *$p<0.05$ WT PVAT; n=5.

Figure 3: A- U46619-induced contraction was not significantly different in WT and KO thoracic aorta rings in the absence of PVAT. In vessels with attached PVAT, there was a significant reduction in contraction in WT but not KO aortic rings. (n=7; *$p<0.05$ and ***$p<0.001$). B- The presence of PVAT significantly augmented the relaxation to chromakalim in WT aortic rings (n=7; ***$p<0.001$ vs. PVAT(-)). C- In aortic rings from AMPKα1 KO mice, the presence of PVAT had no effect on relaxation to cromakalim (n=7).

Figure 4: In cross-over experiments using aortic rings without PVAT, addition of WT PVAT enhanced cromakalim induced relaxation in KO aortic rings (A). However, addition of KO PVAT to WT aortic rings (B) did not significantly alter the relaxation to cromakalim (n=6; ***$p<0.001$ vs. PVAT(-). Conditioned media from WT aortic PVAT significantly enhanced relaxation to cromakalim (C) while KO conditioned media had no effect on relaxation to cromakalim (D). (n=6; ***$p<0.001$ vs. PVAT(-).

Figure 5: Adiponectin concentration of conditioned media from WT and KO mice determined using an ELISA kit. WT PVAT released significantly more adiponectin than KO PVAT (**$p<0.01$; n =5).

Figure 6: A- Incubation of WT aortic rings without PVAT with 1µg mL^{-1} globular adiponectin significantly augmented relaxation to cromakalim. In KO mice, incubation with globular adiponectin significantly enhanced relaxation to cromakalim in aortic rings without PVAT (B) and also in rings where the PVAT was intact (C). (n =5, ***$p < 0.001$ vs. PVAT(-)).

Figure 7: In aortic rings with intact PVAT, addition of 5µg mL^{-1} of the adiponectin receptor 1 (AdipoR1) blocking peptide significantly attenuated relaxation to cromakalim in WT mice (A) but had no effect in rings from KO mice (B). (n =6, ***$p < 0.001$ vs PVAT(+)).

Supplementary Figures

Figure S1: Brown adipose tissue marker (UCP-1) present in different depots of adipose tissue from both wild type and AMPKα_1 knockout mice. Representative histological sections of brown adipose tissue (BAT) (A&B), white adipose tissue (WAT)(C&D), thoracic PVAT (E&F), abdominal PVAT (G&H) and mesenteric PVAT (I&J) stained with anti UCP-1 and counterstained with haematoxylin. Positive immunoreactivity for UCP-1 is indicated by brown colour. **(**AO= aorta, MA= mesenteric artery, scale bar 20 μm, magnification x20)

Figure S2: Brown adipose tissue marker (UCP-1) expression in different PVAT depots. UCP-1 expression was divided by GAPDH to adjust for protein loading. Western blots were performed in BAT (brown adipose tissue); WAT (white adipose tissue); TA (thoracic artery PVAT); AA (abdominal aorta PVAT); MES (mesenteric artery PVAT) from WT and KO homogenates. Blot shown are representative n=3 for all groups.

Figure S3: AMPK expression and activity in cultured rat aortic vascular smooth muscle cells (VSMCs). VSMCs samples were treated with AICAR and cromakalim, lysed and immunoblotting was performed. Graphs are expressed as the fold-change of the phosphorylated form of each enzyme divided by the total AMPKα (B) or total ACC (C) to measure the activation of the enzyme. Blots shown are representative; n=3 for all groups.

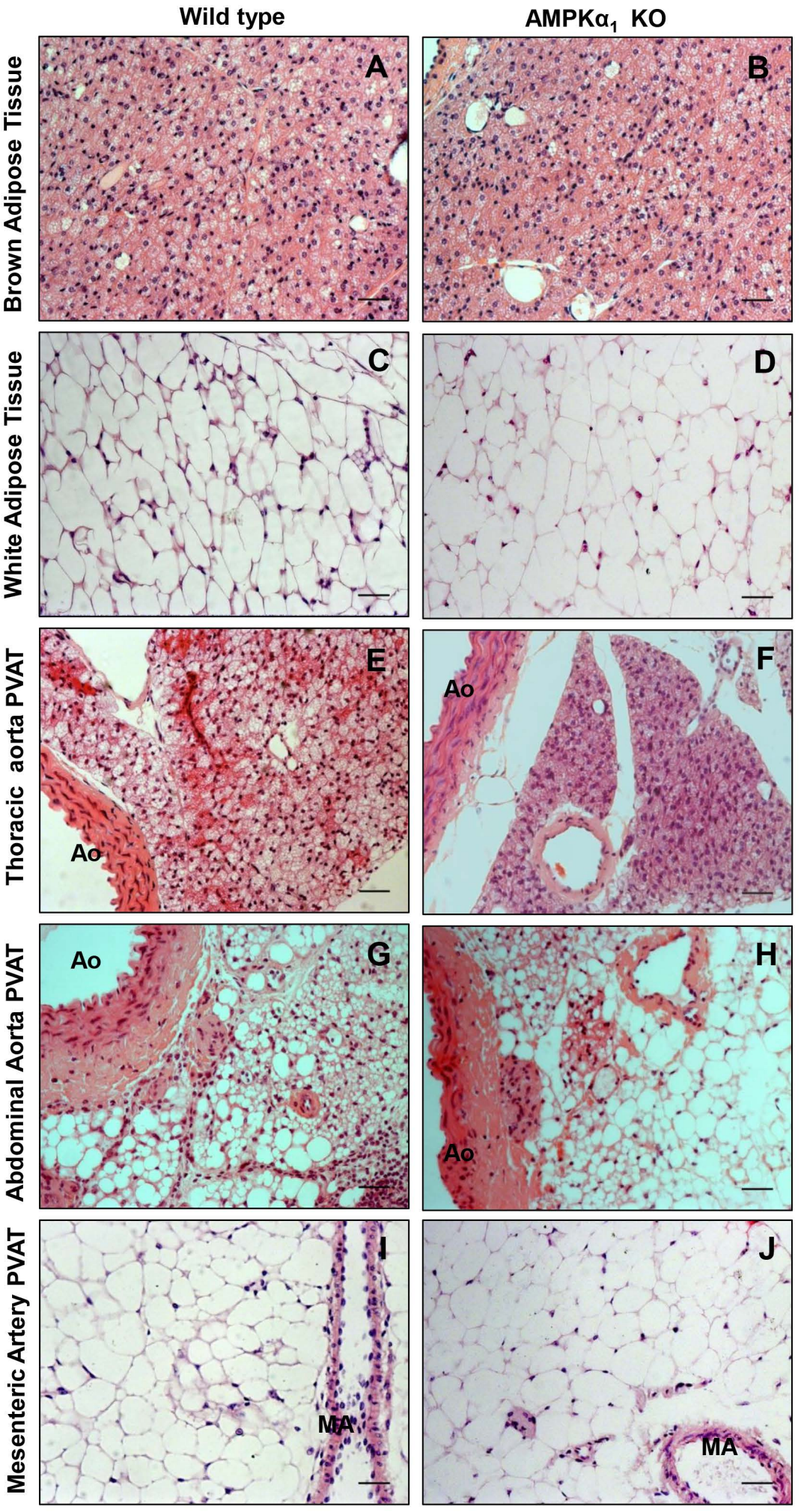
Wild type
AMPKα1 KO
Brown Adipose Tissue
White Adipose Tissue
Thoracic aorta PVAT
Abdominal Aorta PVAT
Mesenteric Artery PVAT
A
B
C
D
E
F
G
H
I
J
Ao
Ao
Ao
Ao
MA
MA

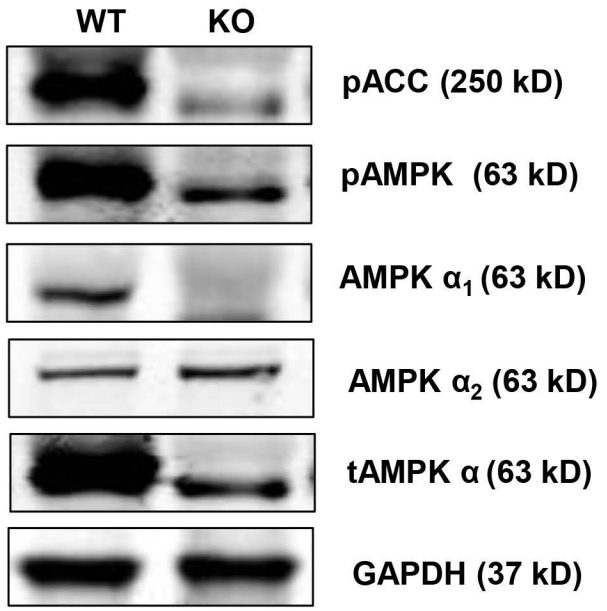
A
WT
KO
pACC (250 kD)
pAMPK (63 kD)
AMPK α1 (63 kD)
AMPK α2 (63 kD)
tAMPK α (63 kD)
GAPDH (37 kD)

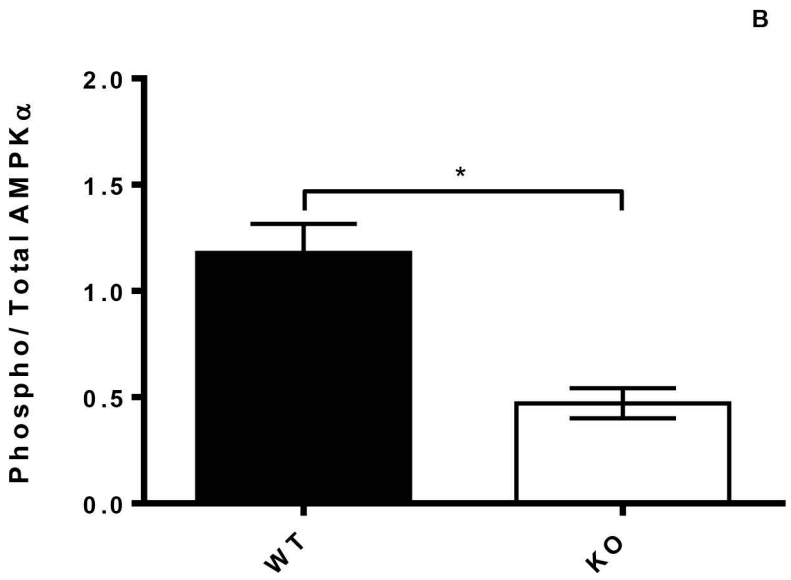
B
Phospho/Total AMPKα
2.0
1.5
1.0
0.5
0.0
*
WT
KO

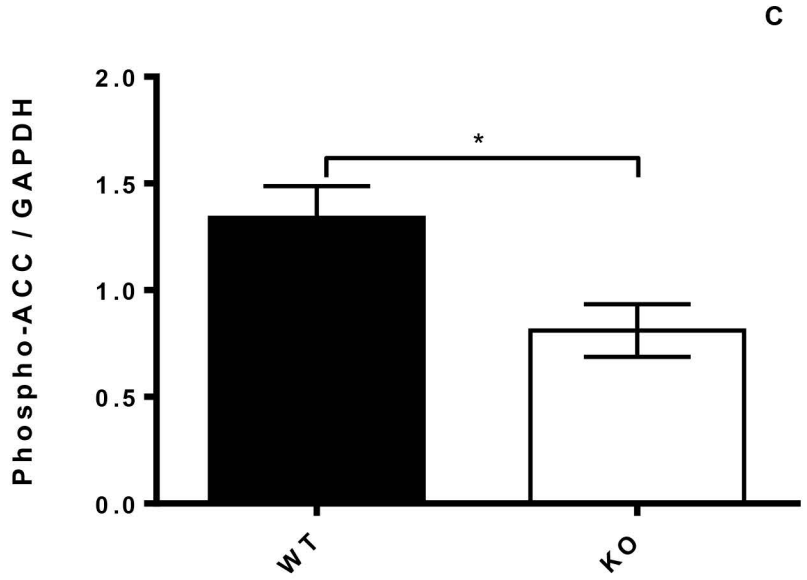
C
Phospho-ACC / GAPDH
2.0
1.5
1.0
0.5
0.0
*
WT
KO

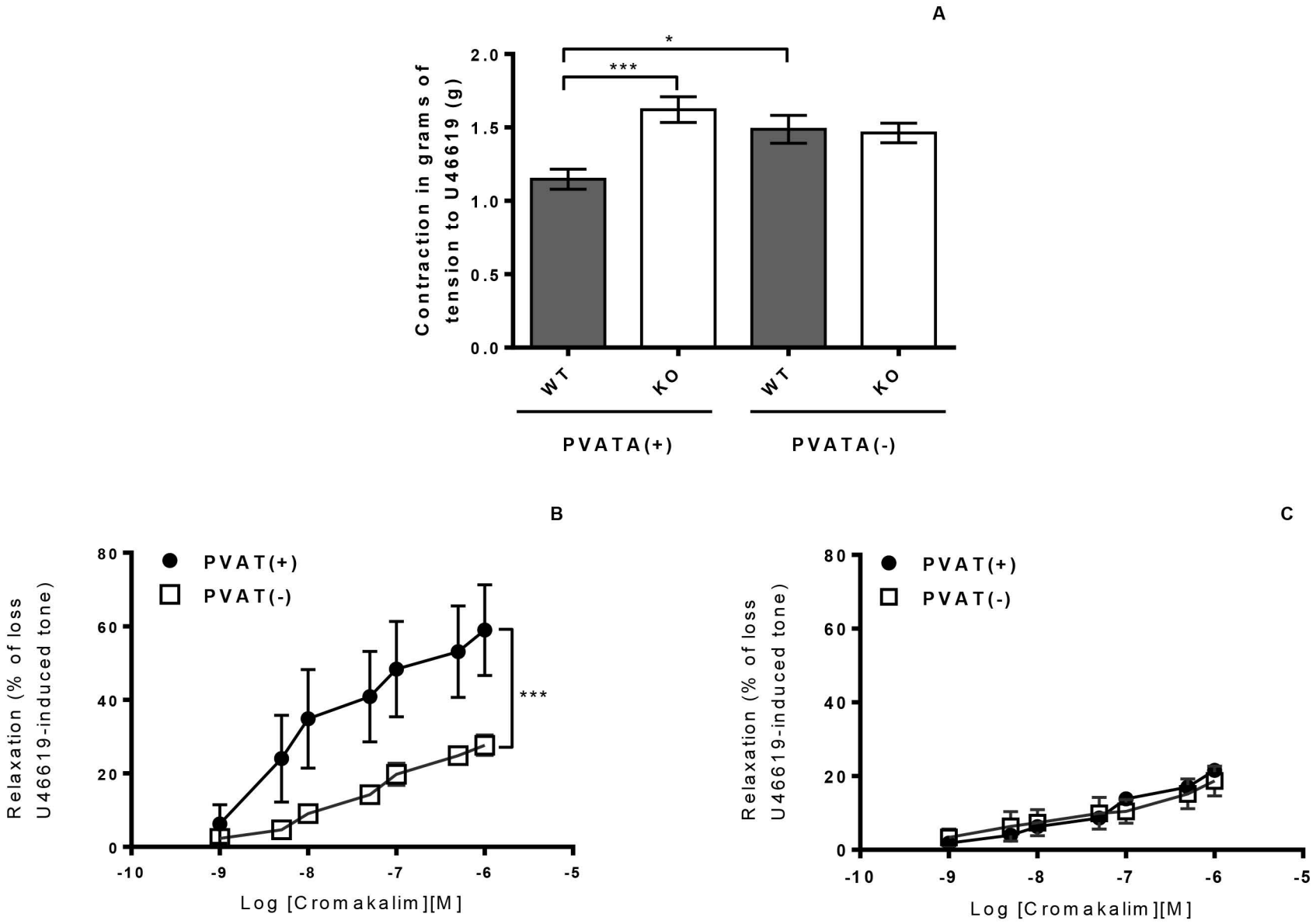
A
Contraction in grams of tension to U46619 (g)
2.0
1.5
1.0
0.5
0.0
*
***
WT
KO
WT
KO
PVATA(+)
PVATA(-)
B
Relaxation (% of loss U46619-induced tone)
80
60
40
20
0
PVAT(+)
PVAT(-)
***
-10
-9
-8
-7
-6
-5
Log [Cromakalim][M]
C
Relaxation (% of loss U46619-induced tone)
80
60
40
20
0
PVAT(+)
PVAT(-)
-10
-9
-8
-7
-6
-5
Log [Cromakalim][M]

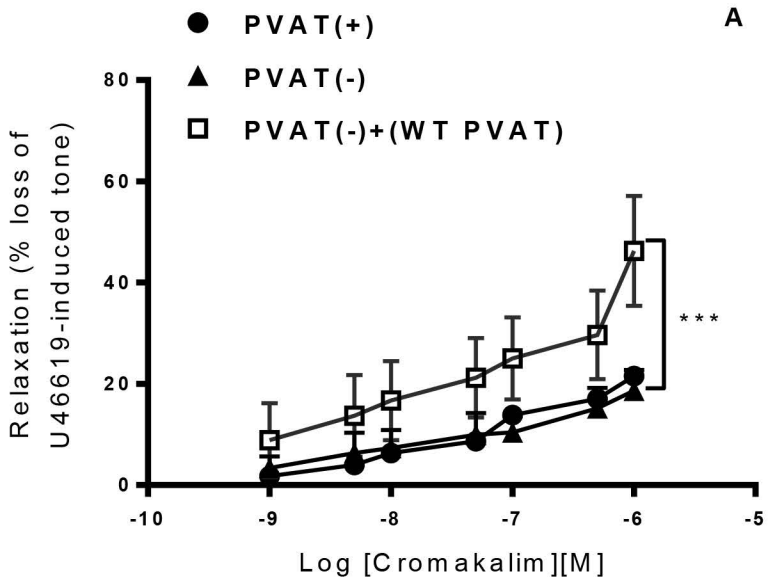
A
PVAT(+)
PVAT(-)
PVAT(-)+(WT PVAT)
Relaxation (% loss of U46619-induced tone)
Log [Cromakalim][M]
***

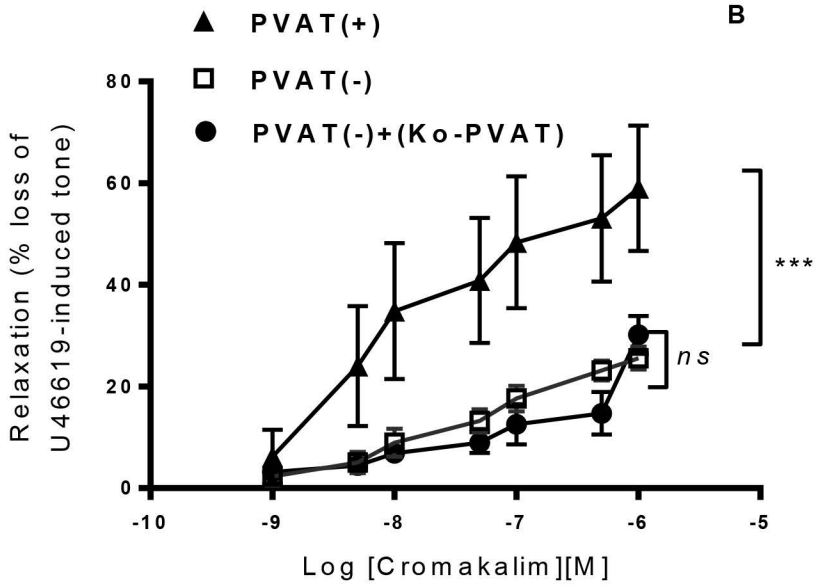
B
PVAT(+)
PVAT(-)
PVAT(-)+(Ko-PVAT)
Relaxation (% loss of U46619-induced tone)
Log [Cromakalim][M]
***
ns

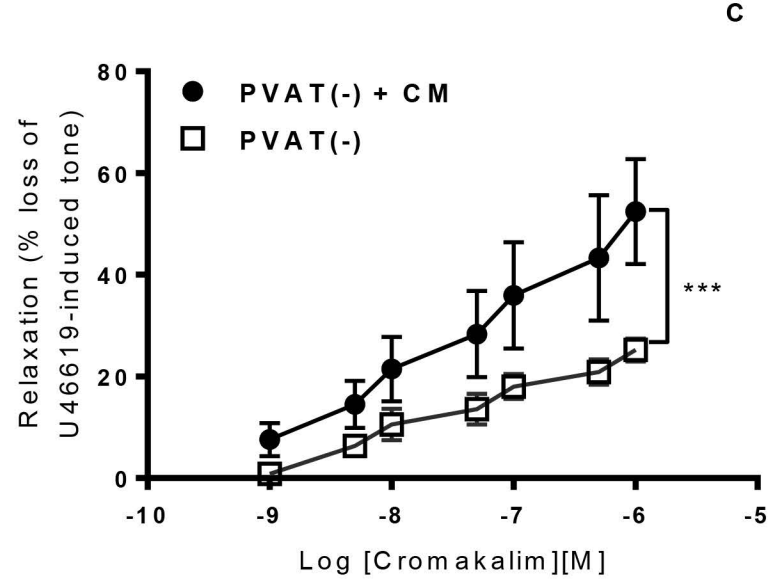
C
PVAT(-) + CM
PVAT(-)
Relaxation (% loss of U46619-induced tone)
Log [Cromakalim][M]
***

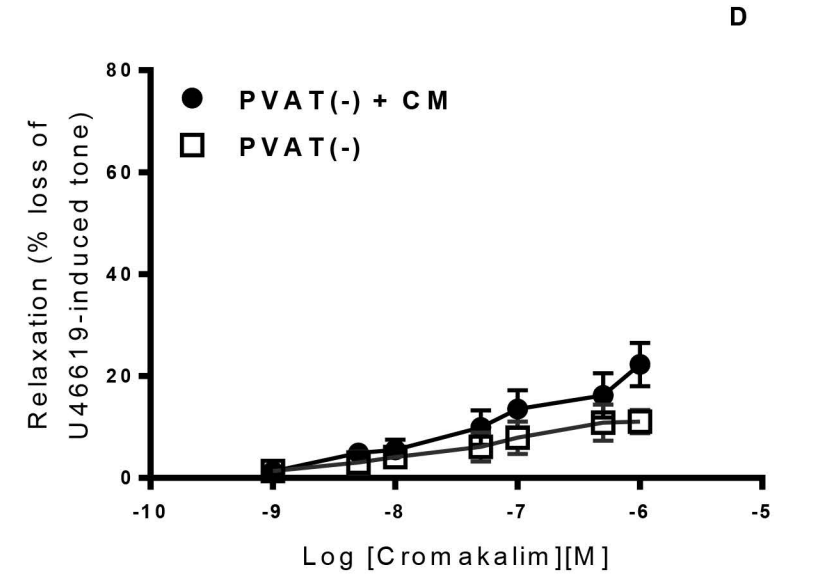
D
PVAT(-) + CM
PVAT(-)
Relaxation (% loss of U46619-induced tone)
Log [Cromakalim][M]

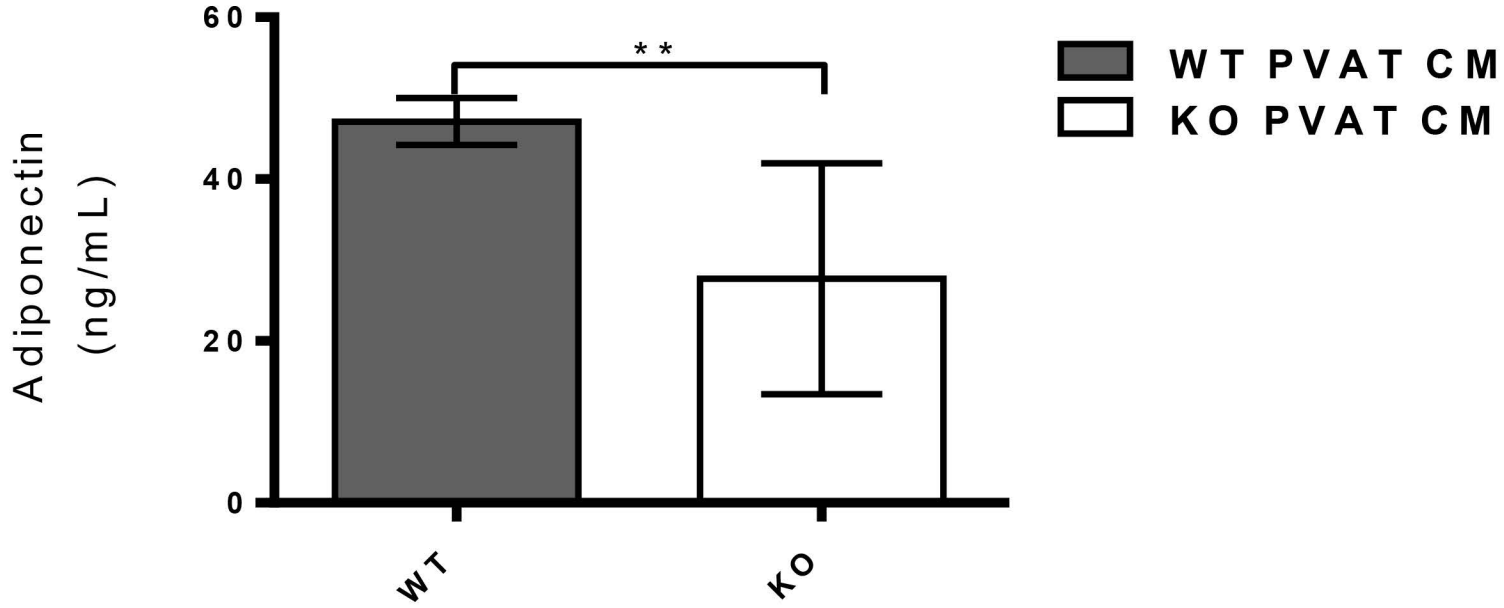
Adiponectin
(ng/mL)
60
40
20
0
**
WT
KO
WT PVAT CM
KO PVAT CM

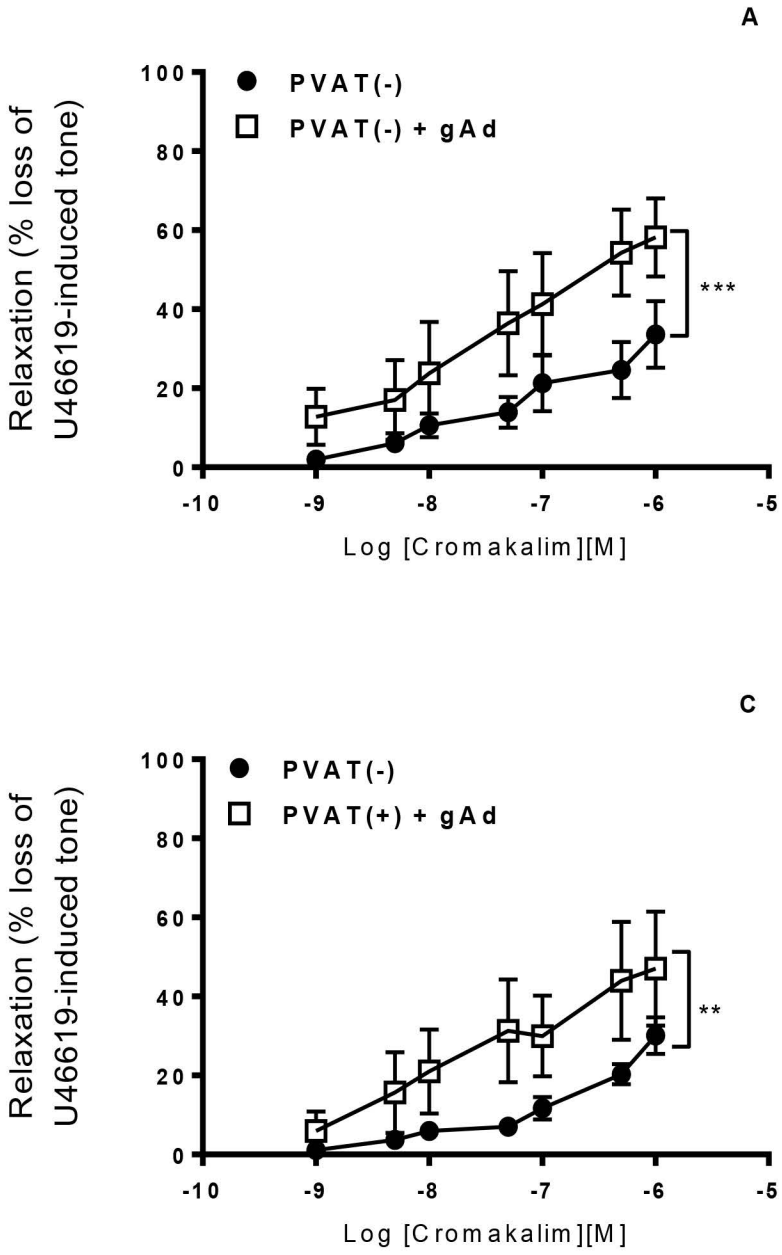
A
B
C
PVAT(-)
PVAT(-) + gAd
PVAT(+) + gAd
Relaxation (% loss of U46619-induced tone)
Log [Cromakalim][M]
***
**
100
80
60
40
20
0
-10
-9
-8
-7
-6
-5

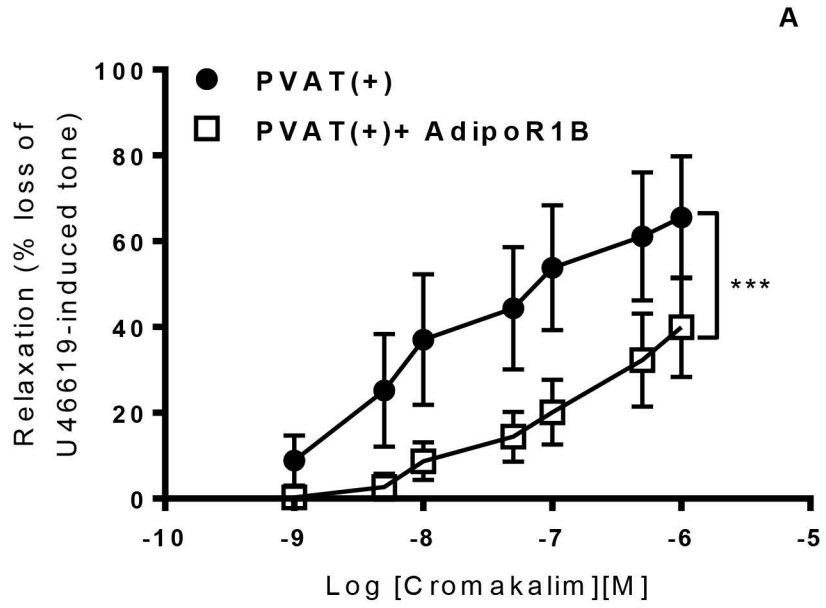
A
PVAT(+)
PVAT(+)+ AdipoR1B
Relaxation (% loss of U46619-induced tone)
100
80
60
40
20
0
-10
-9
-8
-7
-6
-5
Log [Cromakalim][M]
***

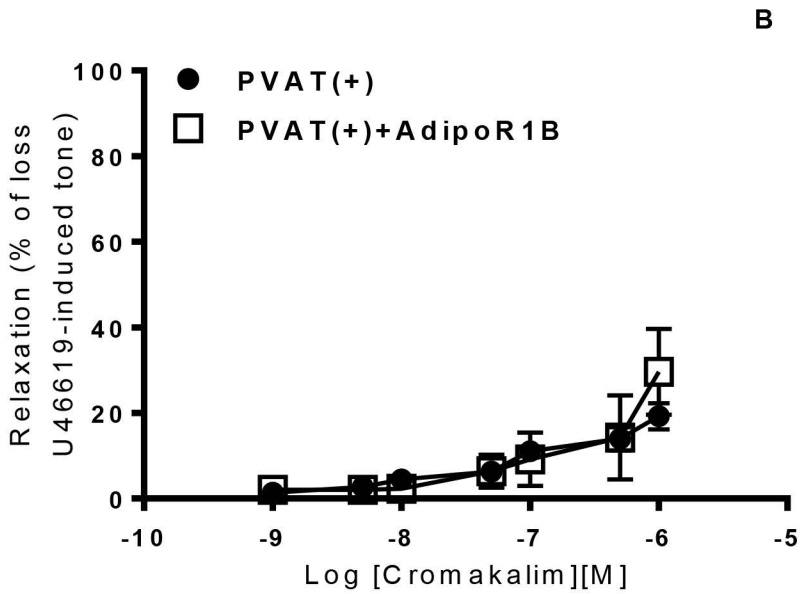
B
PVAT(+)
PVAT(+)+AdipoR1B
Relaxation (% of loss U46619-induced tone)
100
80
60
40
20
0
-10
-9
-8
-7
-6
-5
Log [Cromakalim][M]

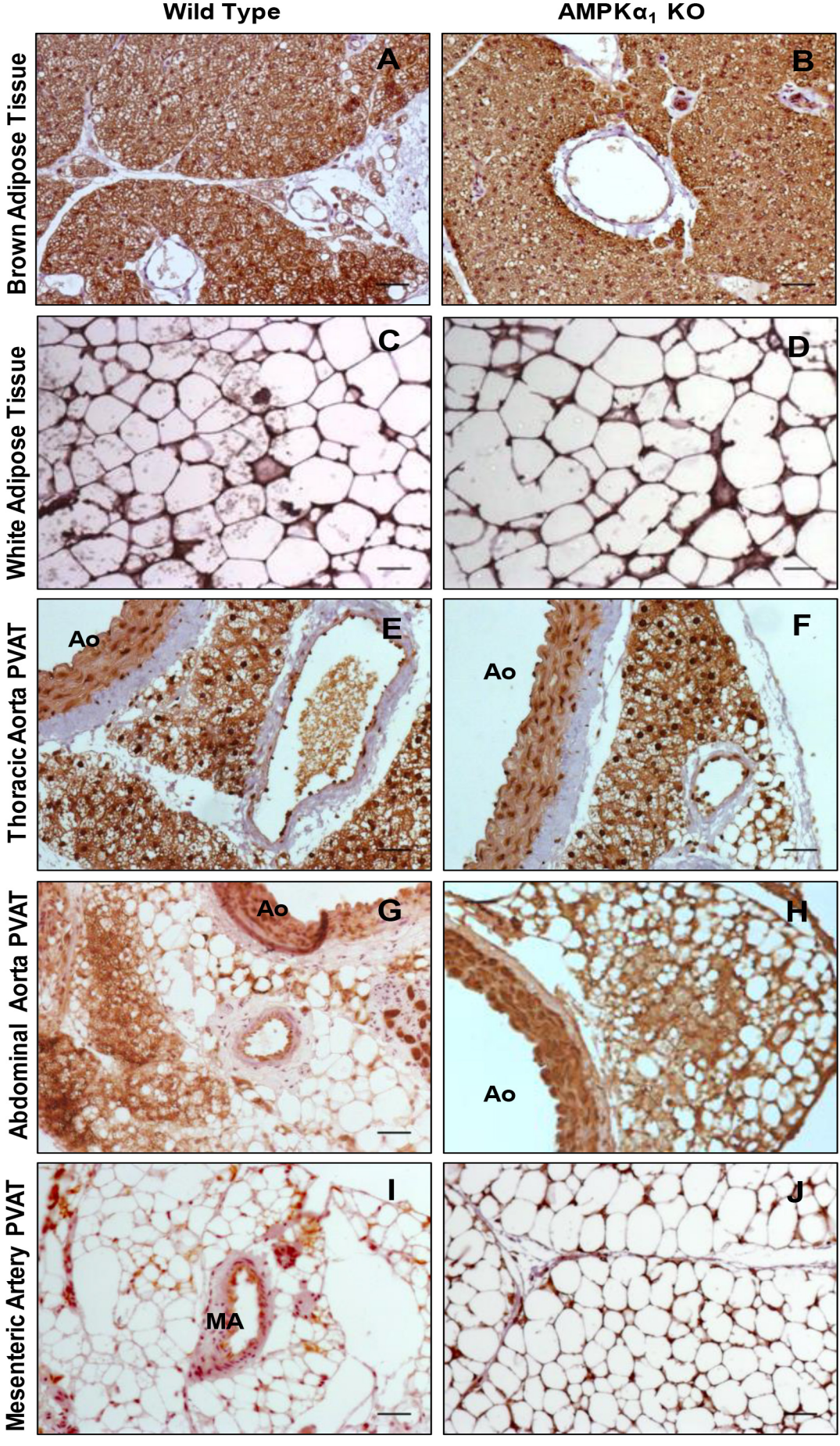
Wild Type
AMPKα1 KO
Brown Adipose Tissue
White Adipose Tissue
Thoracic Aorta PVAT
Abdominal Aorta PVAT
Mesenteric Artery PVAT
A
B
C
D
E
F
G
H
I
J
Ao
Ao
Ao
Ao
MA

A

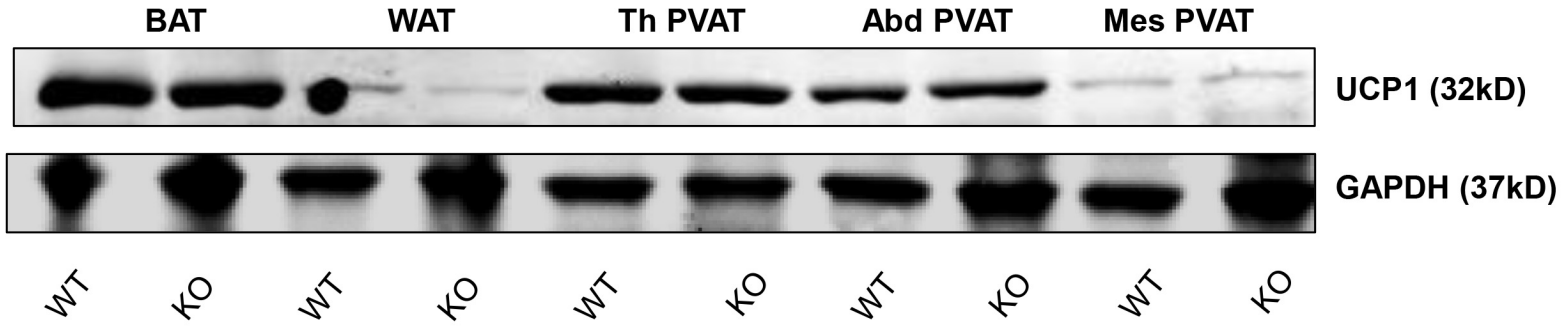
BAT
WAT
Th PVAT
Abd PVAT
Mes PVAT
UCP1 (32kD)
GAPDH (37kD)
WT
KO
WT
KO
WT
KO
WT
KO
WT
KO

B

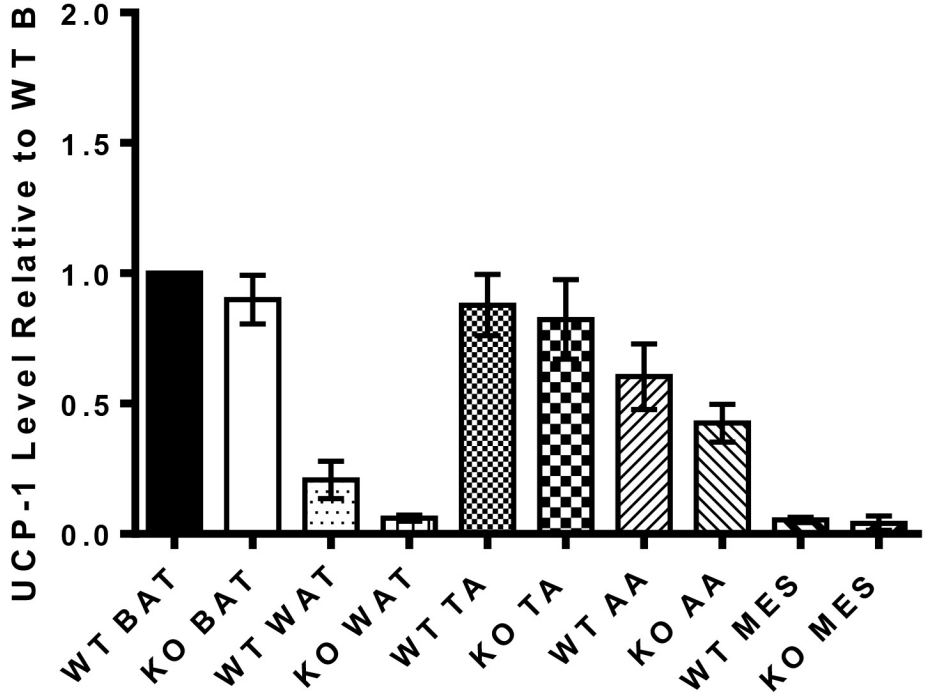
UCP-1 Level Relative to WT BAT
2.0
1.5
1.0
0.5
0.0
WT BAT
KO BAT
WT WAT
KO WAT
WT TA
KO TA
WT AA
KO AA
WT MES
KO MES

A

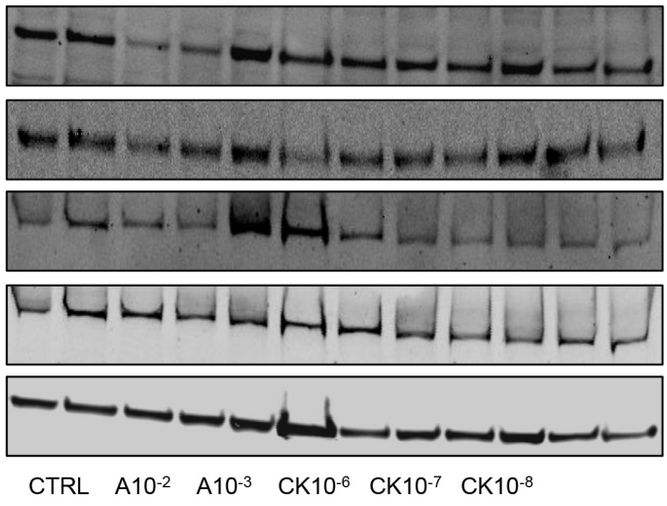
pAMPK-α (63 kDa)
tAMPK-α (63 kDa)
pACC (280 kDa)
tACC (280 kDa)
α-Actin (42 kDa)
CTRL
A10-2
A10-3
CK10-6
CK10-7
CK10-8

B

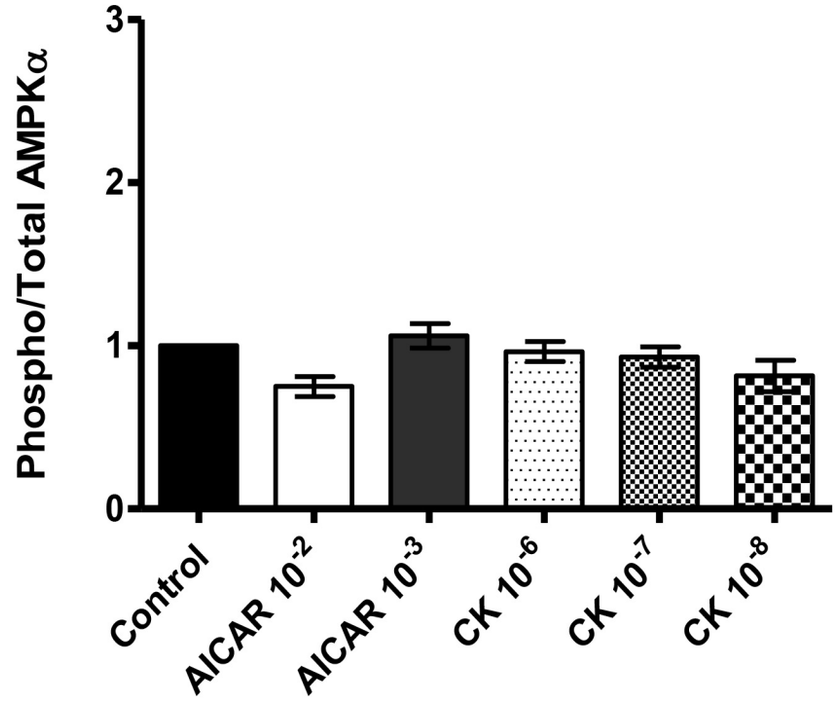
Phospho/Total AMPKα
3
2
1
0
Control
AICAR 10-2
AICAR 10-3
CK 10-6
CK 10-7
CK 10-8

C

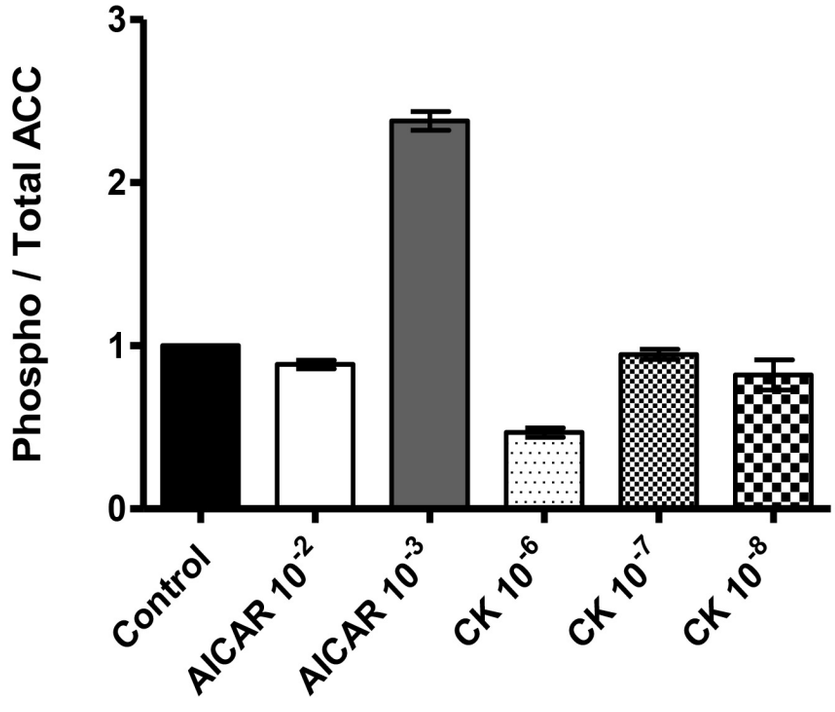
Phospho / Total ACC
3
2
1
0
Control
AICAR 10-2
AICAR 10-3
CK 10-6
CK 10-7
CK 10-8